PAPER • OPEN ACCESS

Hard X-ray USAXS Fourier Transform Holography

To cite this article: W Roseker *et al* 2022 *J. Phys.: Conf. Ser.* **2380** 012118

Hard X-ray USAXS Fourier Transform Holography

W Roseker[1], W Jo[1,3], R Rysov[1], F Westermeier [1], L Bocklage[1,2], M Riepp[1], A Philippi-Kobs[1], L Müller[1], M Walther[1], M Sprung[1] and G Grübel[1,2]

[1]Deutsches Elektronen-Synchrotron DESY, Notkestr. 85, 22607 Hamburg, Germany
[2]The Hamburg Centre for Ultrafast Imaging, Luruper Chaussee 149, 22761 Hamburg, Germany
[3]Present address: European XFEL, Holzkoppel 4, 22869 Schenefeld, Germany

E-mail: wojciech.roseker@desy.de

Abstract. We report on a Fourier transform holography study, employing hard X-ray energies at a 3rd generation storage ring. Nano-structures of various sizes and shapes have been measured in ultra small angle x-ray scattering configuration reaching a resolution in the holographic reconstructions of about 50 nm. Reliable holograms have been obtained with 6.9×10^6 incident photons. Our results provide an important step forward towards routine split-pulse Fourier transform holography measurements at FEL sources and 4th generation ultralow-emittance sources.

1. Introduction

Lensless coherent X-ray imaging became one key techniques at Free Electron Lasers (FELs) and storage rings suited for high resolution microscopy. Examples include coherent diffractive imaging (CDI) on nanoscales [1, 2], Fourier transform holography (FTH) from magnetic domains [3, 4, 5], in-line X-ray holography [6], and in-flight holography [7]. Coherent X-ray imaging techniques strongly rely on a high degree of transverse coherence. Although the phase information is lost by recording the diffraction intensities by the detector, it can still be retrieved by computational means. CDI requires iterative algorithms to retrieve the phase information [8]. In contrast, the lensless FTH approach employs well-defined reference objects. The interference of the scattered waves from the sample and from reference objects generates a hologram. The image of the sample structure is obtained by a simple Fourier transform. In recent years FTH was developed into a robust technique with soft X-rays [3, 9, 10, 11]. The feasibility of hard X-ray FTH imaging combined with CDI was demonstrated with spatial resolution of 25 nm [12]. Further attempts of hard X-ray FTH have been very limited. Combining FTH with the split-and-delay technique [13, 14, 15, 16, 17] at FEL sources opened the possibility to measure dynamics with femtoseconds resolution [18]. In this way FTH was employed to measure X-ray holograms using a soft X-ray autocorrelator, where FEL pulses were geometrically separated and split into two with femtoseconds delay to overlap on the sample position. The diffraction patterns generated from both pulses were separated on the detector and could thus be treated independently. However, due to the use of soft X-rays the maximum achievable wave-vector transfer and the spatial resolution is limited which can be improved significantly using hard X-rays.

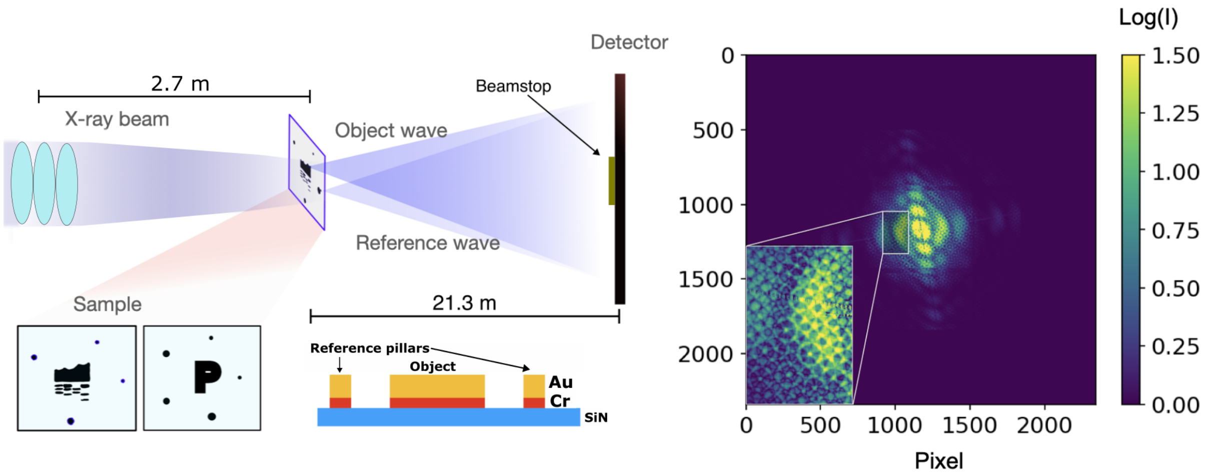

Figure 1. (Top left) Sketch of the Fourier Transform Holography technique at the beamline P10 of PETRA III. (Bottom left) Sketch of the samples and their corresponding cross section. (Right) Recorded hologram image obtained from the sample object *letter P* and reference pillars shown in Fig. 2a). The inset shows the details of the interference pattern originating from the sample object and multiple reference pillars.

Here we demonstrate hard X-ray FTH measurements in ultra small-angle X-ray scattering (USAXS) configuration on nano to micrometer sized objects. In our study, we aimed to determine the spatial resolution and the required photon flux for successful hard X-ray FTH reconstructions.

2. Experimental

The experiment was performed at the coherence applications beamline P10 of PETRA III [19]. The experiment was carried out at 8.6 keV photon energy. The beam size b_S at the sample position was defined by compound refractive lenses (CRLs) to about $5\times6\,\mu m^2$ (vertical × horizontal). The beamlime was set up in the so-called USAXS configuration providing a sample to detector distance $L = 21.3$ m. A sketch of the experiment is presented in Fig. 1. The holograms were recorded by an Eiger-4M detector. A semitransparent silicon beamstop has been used, which features a central 500 µm round tantalum disc to stop the direct beam. The use of the beamstop allowed to retrieve the scattering intensity at very low q values. The resolution of the hologram reconstruction is defined by the speckle size Δ_s, the reference structures (i.e, "positive" sub-micron objects called pillars) size Δ_r and the maximum q values reached in the experiment according to $\Delta_q = \pi/q_{\max} = 20$ nm. The speckle size was much larger than the pixel size of the detector, i.e, 75 µm. The speckle size was obtained via $d_s = \lambda L/b_s = 307\,\mu m$, where λ is the X-ray wavelength.

The sample objects were prepared in various shapes and sizes by e-beam lithography, sputter deposition and ion beam etching. A 10 nm Cr/90 nm Au bilayer was deposited onto 200 nm thick silicon nitride membranes (see Fig. 1). A negative resist atop was structured by e-beam lithography. All excess metal was removed by Ar ion−beam etching. The residual resist was removed by an oxygen plasma, leaving only the metallic structures on the silicon nitride membrane. Scanning electron microscopy images of the samples, i.e. the *letter P* and a stylized version of the Elbphilharmonie (*Elphi*) are shown in Fig. 2a) and Fig. 3a), respectively. The smallest reference pillars are approximately 80 nm in diameter.

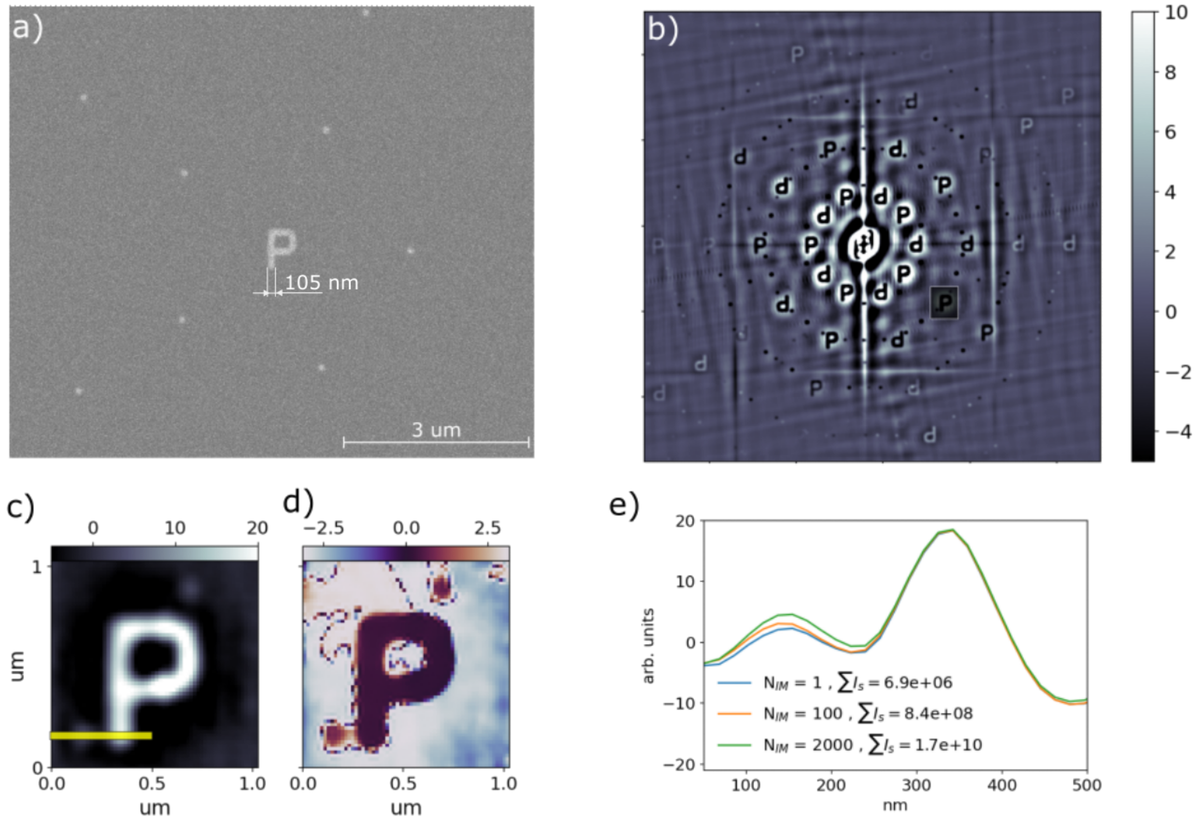

Figure 2. a) SEM image of the sample *letter P* and reference pillars. b) Reconstruction of the hologram showing the sample object letter P and reference pillar structures. c) Zoom into the reconstruction denoted by the dark rectangle in b) and d) its corresponding phase. e) Line-cut through the smallest feature of letter P and reference pillar structure marked by the yellow line in c).

3. Results and Discussion

Figure 1 shows an FTH image recorded in the far field and corrected for background scattering. The hologram shows the interference pattern from the sample object and multiple reference pillars. Figure 2a) shows the SEM image of the sample *letter P* surrounded by reference objects (pillars) that were placed on 5 concentric circles with radii of multiples of $r_R = 2\,\mu m$. The narrowest part of the sample is 105 nm as depicted with the white arrows in Fig. 2a). FTH hologram records information on the auto-correlation terms and the cross-correlation terms between the sample and the reference objects and its complex conjugate, i.e., a 180° rotated copy. Figure 2b) shows the resulting reconstruction of the sample object *letter P* and the reference pillar structures. The auto-correlation terms are visible in the central part of the image. More than 30 cross-correlation terms of the sample and references can be seen in the reconstruction. Figure 2c) shows a region-of-interest (ROI) that corresponds to the selected image of the sample. The sample object shape, i.e. *letter P*, is clearly recognizable. The line-cut through the ROI, shown in Fig. 2e), indicates that one can resolve structures of about 100 nm. Figure 2d) presents the retrieved phases. As the object's phase is uniform it indicates the homogeneity of the sample height. The hologram image is the result of 1 s acquisition time with $N = 6.9{\times}10^6$ incident photons at the sample position. The incident flux is comparable to a single FEL pulse intensity transmitted thought a split-and-delay optics [17] indicating the

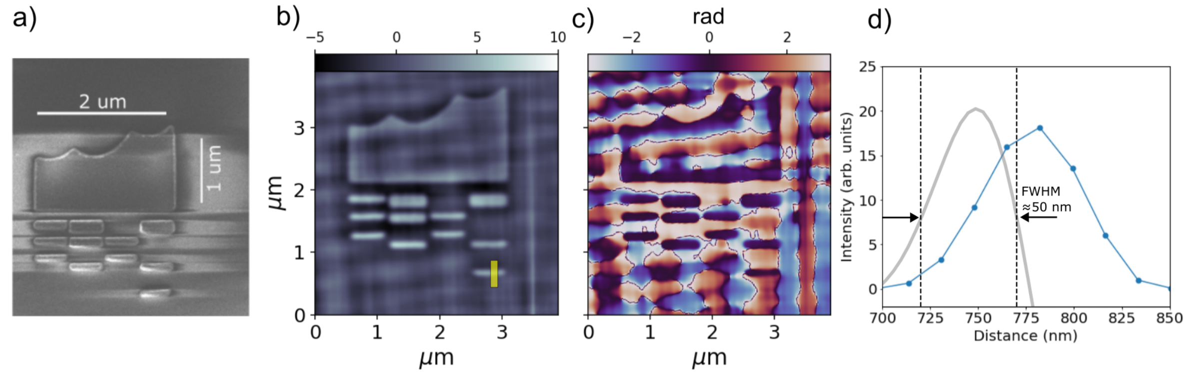

Figure 3. a) SEM image of the sample and the reference objects. b) Reconstructed test structure from the hologram image and c) the corresponding phase. d) Line-cut through the smallest feature marked by the yellow line in b) indicating a resolution of $\approx$ 50 nm (see the vertical dashed lines). Grey line denotes a numerical differentiation of the line-cut profile.

feasibility of hard X-ray split-pulse FTH imaging. Increasing the photon number to $1.7{\times}10^{10}$ does not improve the spatial resolution of the reconstruction, as shown in Fig. 2e).

Figure 3 presents the results from the FTH study on a larger sample object with dimensions of $\approx 2 \times 2\,\mu$m. Figure 3b) depicts the FTH reconstructed image of the *Elphi* object. Line-cut through the smallest feature of the reconstruction marked by a yellow rectangle, indicates the resolution of $\approx 50\,$nm. The value was obtained from a FWHM of the a numerical differentiation of the line-cut profile, denoted by vertical dash lines as shown in Fig. 3d). Strong variations of phases, mostly caused by the missing pixels due to the beamstop and the edges of the semi-transparent beamstop, are clearly visible in Fig. 3c). These spatial frequencies are absent for smaller samples (see Fig. 2d))

4. Conclusions
In conclusion we have shown FTH imaging in USAXS configuration with hard X-rays. Successful holographic reconstructions show that all the sample features could be resolved with a resolution of $\approx 50\,$nm without phase retrieval algorithms. Holographic reconstructions were obtained with $6.9{\times}10^{6}$ photons, indicating the feasibility of split-pulse FTH experiments at FEL sources. These results are very relevant in light of future studies on time-resolved molecular, biological and chemical processes, reaction dynamics and molecular dynamics via split-pulse FTH imaging at X-ray FEL sources. Moreover, the potential of reaching high spatial resolution and femtosecond time scales to track, e.g., the evolution of radiation damage on ultrashort time scales, will stimulate new developments in theory and establish new bridges between experiment and theory.

5. Acknowledgments
We acknowledge the support of the Clusters of Excellence “The Hamburg Centre for Ultrafast Imaging” and “Advanced Imaging of Matter” of the Deutsche Forschungsgemeinschaft (DFG) (EXC 1074 - project ID 194651731, and EXC 2056 - project ID 390715994). We acknowledge DESY (Hamburg, Germany), a member of the Helmholtz Association HGF, for the provision of experimental facilities. Parts of this research were carried out at PETRA III. We would also like to acknowledge support by DFG – SFB-925 – project 170620586. We would like to thank L. Stadler for fruitful discussions.

References

[1] Chapman H N, Barty A, Bogan M J, Boutet S, Frank M, Hau-Riege S P, Marchesini S, Woods B W, Bajt S, Benner W H, London R A, Plönjes E, Kuhlmann M, Treusch R, Düsterer S, Tschentscher T, Schneider J R, Spiller E, Möller T, Bostedt C, Hoener M, Shapiro D A, Hodgson K O, van der Spoel D, Burmeister F, Bergh M, Caleman C, Huldt G, Seibert M M, Maia F R N C, Lee R W, Szöke A, Timneanu N and Hajdu J 2006 *Nature Physics* **2** 839

[2] Barty A, Boutet S, Bogan M J, Hau-Riege S, Marchesini S, Sokolowski-Tinten K, Stojanovic N, Tobey R, Ehrke H, Cavalleri A, Düsterer S, Frank M, Bajt S, Woods B W, Seibert M M, Hajdu J, Treusch R and Chapman H N 2008 *Nature Photonics* **2** 415

[3] Eisebitt S, Lüning J, Schlotter W F, Lörgen M, Hellwig O, Eberhardt W and Stöhr J 2004 *Nature* **432** 885

[4] Tieg C, Frömter R, Stickler D, Hankemeier S, Kobs A, Streit-Nierobisch S, Gutt C, Grübel G and Oepen H P 2010 *Optics Express* **18** 27251

[5] Duckworth T A, Ogrin F, Dhesi S S, Langridge S, Whiteside A, Moore T, Beutier G and van der Laan G 2011 *Optics Express* **19** 16223

[6] Soltau J, Vassholz M, Osterhoff M and Salditt T 2021 *Optica* **8** 818

[7] Gorkhover T, Ulmer A, Ferguson K, Bucher M, Maia F R N C, Bielecki J, Ekeberg T, Hantke M F, Daurer B J, Nettelblad C, Andreasson J, Barty A, Bruza P, Carron S, Hasse D, Krzywinski J, Larsson D S D, Morgan A, Mühlig K, Müller M, Okamoto K, Pietrini A, Rupp D, Sauppe M, van der Schot G, Seibert M, Sellberg J A, Svenda M, Swiggers M, Timneanu N, Westphal D, Williams G, Zani A, Chapman H N, Faigel G, Möller T, Hajdu J and Bostedt C 2018 *Nature Photonics* **12** 150

[8] Miao J, Sayre D and Chapman H 1998 *Journal of the Optical Society of America, Part A: Optics and Image Science* **15** 1662

[9] Schlotter W F, Rick R, Chen K, Scherz A, Stöhr J, Lüning J, Eisebitt S, Günther C, Eberhardt W, Hellwig O and McNulty I 2006 *Applied Physics Letters* **89** 163112

[10] Schlotter W F, Lüning J, Rick R, Chen K, Scherz A, Eisebitt S, Günther C M, Eberhardt W, Hellwig O and Stöhr J 2007 *Optics Letters* **32** 3110

[11] Marchesini S, Boutet S, Sakdinawat A E, Bogan M J, Bajt S, Barty A, Chapman H N, Frank M, Hau-Riege S P, Szöke A, Cui C, Shapiro D A, Howells M R, Spence J C, Shaevitz J W, Lee J Y, Hajdu J and Seibert M M 2008 *Nature Photonics* **2** 560

[12] Stadler L M, Gutt C, Autenrieth T, Leupold O, Rehbein S, Chushkin Y and Grübel G 2008 *Physical Review Letters* **100** 245503

[13] Li H, Sun Y, Sutton M, Fuoss P and Zhu D 2020 *Optics Letters* **45** 2086

[14] Roling S, Kärcher V, Samoylova L, Appel K, Braun S, Gawlitza P, Siewert F, Zastrau U, Rollnik M, Wahlert F and Zacharias H 2017 vol 10237 (SPIE) p 1023713

[15] Mitzner R, Siemer B, Neeb M, Noll T, Siewert F, Roling S, Rutkowski M, Sorokin A, Richter M, Juranic P, Tiedtke K, Feldhaus J, Eberhardt W and Zacharias H 2008

[16] Osaka T, Hirano T, Morioka Y, Sano Y, Inubushi Y, Togashi T, Inoue I, Tono K, Robert A, Yamauchi K, Hastings J B and Yabashi M 2017 *IUCrJ* **4** 728

[17] Roseker W, Hruszkewycz S O, Lehmkühler F, Walther M, Schulte-Schrepping H, Lee S, Osaka T, Strüder L, Hartmann R, Sikorski M, Song S, Robert A, Fuoss P H, Sutton M, Stephenson G B and Grübel G 2018 *Nature Communications* **9** 1704

[18] Günther C M, Pfau B, Mitzner R, Siemer B, Roling S, Zacharias H, Kutz O, Rudolph I, Schondelmaier D, Treusch R and Eisebitt S 2011 *Nature Photonics* **5** 99

[19] Zozulya A, Shabalin A, Schulte-Schrepping H, Heuer J, Spiwek M, Sergeev I, Besedin I, Vartanyants I A and Sprung M 2014 *Journal of Physics: Conference Series* **499** 012003